(Received 4 August 2024, Accepted 25 September 2024, Scheduled 7 October 2024)

Wearable Wideband Textile Coplanar Vivaldi Antenna for Medical and IoT Application

Nurhayati Nurhayati[1, *], Agam N. D. N. Fahmi[1], Pradini Puspitaningayu[1], Oce Wiriawan[2], Brian Raafi'u[3], Fitri A. Iskandarianto[3], Ahmed J. A. Al-Gburi[4], Atul Varshney[5], and Safpbri Johari[6]

[1]*Department of Electrical Engineering, Universitas Negeri Surabaya, Surabaya 60231, Indonesia*
[2]*Department of Sport Education, Universitas Negeri Surabaya, Surabaya 60213, Indonesia*
[3]*Department of Instrumentation Engineering, Institut Teknologi Sepuluh Nopember, Surabaya 60111, Indonesia*
[4]*Center for Telecommunication Research and Innovation (CeTRI)*
Faculty of Electronics and Computer Technology and Engineering
Universiti Teknikal Malaysia Melaka (UTeM), Melaka 76100, Malaysia
[5]*Electronics and Communication Engineering, FET, Gurukula Kangri (Deemed to be university), Haridwar, Uttarakhand, India*
[6]*Advanced Communication Engineering (ACE) Centre of Excellence, Faculty of Electronic Engineering & Technology*
Universiti Malaysia Perlis (UniMAP), Arau, Perlis, 01000, Malaysia

ABSTRACT: Wearable technologies will be extremely useful in the future life. This research proposes a textile wideband coplanar Vivaldi antenna constructed from a felt substrate and two distinct types of patches, shieldit, and copper tape integrated with a wearable device. This study also altered the slope of the tapered slot on the antenna's front and side to see how it affected the bandwidth and directivity antenna performance. An IoT wearable device that was connected to a microcontroller via a DS18B20 body temperature sensor and a MAX30100 sensor for heart rate and oxygen level monitoring was paired with the textile antenna. Based on the simulation findings, it was discovered that a 1 mm thick felt substrate material combined with a copper tape patch produces a workable frequency range of 2.6 GHz to 8.7 GHz, a minimum S_{11} of -44.93 dB at 3 GHz, and a fractional bandwidth up to 107%. According to the simulation results, the antenna's side and front tapered slots have an impact on directivity and return loss. Directivity at 3 GHz can be raised by 2.63 dBi, from 1.94 dBi to 4.57 dBi, by varying the Vivaldi antenna form on both sides of the patch. The data from the sensor was successfully conveyed by combining an IoT wearable device with a textile antenna. Thus, we deduce that the textile coplanar Vivaldi antenna is appropriate for Internet of Things applications.

1. INTRODUCTION

Implementing a system that can offer health information for first diagnosis can serve as a first step in preventing more serious health concerns, as well as a reference for paramedics in determining the patient's physical state and treatment. Services for monitoring bodily health in real time can be done utilizing Internet of Things (IoT) technology [1–3] or Wireless Bodily Area Network (WBAN) [4–6]. The IoT platform monitors health data by combining numerous sensors such as blood sugar, blood pressure, heart rate, and other vital indicators sensors, with the data-sending process managed by a microcontroller acting as a data transmitter and connecting to an antenna. Monitoring technology has evolved to the point that it is simple for the public to use, hence it is dubbed as a wearable device [7].

The usage of wearable gadget technology has diverse advantages and disadvantages in each category, but it makes a significant contribution to the field of health. The technology used in wearable gadgets relies on a wireless communication system to deliver and receive data. The antenna is the front end of the telecommunications system, hence its performance must be improved. These antennas, effectively incorporated into wearable devices, play an important role in continually and surreptitiously tracking vital indicators. There have been various experiments conducted to increase antenna performance utilizing textile materials.

A rectangular textile antenna of $250 \times 250\,\text{mm}^2$ in size and made of EVA (ethylene-vinyl acetate) foam and copper gauze was investigated in [8]. A wearable PIFA rectangular patch antenna with metasurface technology that can work at frequencies 4.96 to 5.9 GHz has also been created utilizing wool felt and nylon materials [9]. The Electronic Band Gap technique on a rectangular patch antenna with a substrate in the form of felt of 1,002 mm thickness and a patch in the form of a shieldit with dimensions of $67.33 \times 63.22\,\text{mm}^2$ working at a frequency of 2.4 GHz has been studied in [10]. A wearable antenna for WBAN made of an FR4 substrate and copper components with dimensions $55 \times 33\,\text{mm}^2$ and operating at 2.4 GHz with a 3.8% bandwidth has been investigated in [11]. The use of WBAN on patch antennas made of felt and super shieldit materials utilizing metasurface antenna methods with a size of $40 \times 40\,\text{mm}^2$ that can operate at 5.2–8 GHz has also been evaluated in [12]. Button-shaped antennas for wireless power transmission have been explained in [13], and a Y patch slot antenna with dimensions $55 \times 30\,\text{mm}^2$ that functions at a frequency 1.65–3.13 GHz

* Corresponding authors: Nurhayati Nurhayati (nurhayati@unesa.ac.id) and Ahmed Jamal Abdullah Al-Gburi (ahmedjamal@ieee.org).

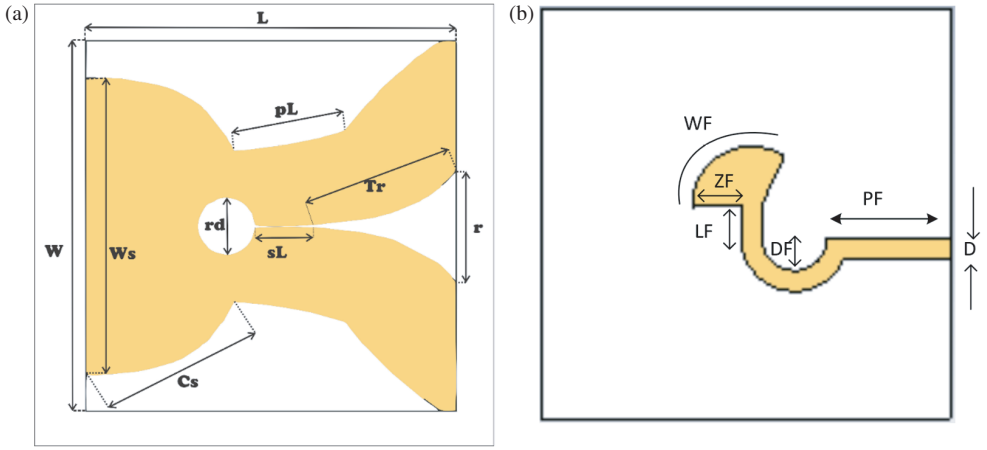

FIGURE 1. Coplanar Vivaldi antenna design (a) front view and (b) bottom view (the feeding).

has been discussed in [14]. A quad-band semiflexible antenna employing Rogers RT5880 has also been explored in [15]. The studies on antennas using textile materials that have been carried out by these researchers have used several layers of substrate and have a complex shape because they use a metasurface structure, electromagnetic band gap (EBG), and have a bandwidth that is not too wide, so it is necessary to develop an antenna that is simple and has a wide bandwidth. There are several textile antenna materials as shown in Table 1.

TABLE 1. Comparison of several flexible antenna types.

Ref.	Textile material	The thickness (mm)	Application
[16]	Cordura	0.5	GPS (1.5 GHz)
[17]	Felt	1.1	WLAN (2.4 GHz)
[18]	Wollen Felt	3.5	Bluetooth (2.4 GHz)
[19]	Polyester	2.8	ISM (2.4 GHz)
[20]	Copper tape	1	WBAN (2.9 GHz)
[21]	Shieldit	6	UWB

The research on textile antennas that can support wearable devices continues to be developed because they can be used for various applications including medicine, sports, military, and IoT. Certain wearable device data transmissions need a lot of bandwidth since they usually require huge capacities of data. Antenna research to increase bandwidth has been carried out on Coplanar Vivaldi Antenna [22, 23], but the antenna substrate material used is still inflexible. So it is necessary to develop an antenna with a wide bandwidth using flexible materials. To develop flexible textile antennas, designers must consider mechanical influences (bending, crumpling, and compression), undesired radiation absorption by human tissue (lower antenna efficiency, potential health hazards when SAR limitations are breached), frequency adjustment, and other factors.

When textile materials are employed in antennas on the human body, certain requirements apply. Specific absorption rate (SAR) value is a key metric to consider during installation. SAR is a measurement of the absorption rate of electromagnetic field distributions that the body may receive. The Federal Communications Commission (FCC) has adopted regulations that limit the dispersion of electromagnetic fields that can be received by the body to around 2 W/kg [24–26]. To ensure that data transfer occurs as efficiently as possible, the antenna which serves as the front end of the transmitter and receiver device must be upgraded further. Aside from its flexibility, antenna performance in terms of operating frequency and radiation pattern has a significant impact on data reception and transmission success. Ultra-wideband (UWB) is a technology developed in 1960 for wearable device purposes. Based on the FCC in 2002, UWB is a wireless technology that is often used by the public. UWB technology can be applied to the antenna to maximize the data connection rate for wireless data transmission using both Bluetooth and WLAN networks [27, 28]. This research also develops a wearable device using a textile Coplanar Vivaldi antenna which can work over a wide bandwidth. The antenna is built into a wearable device that is coupled to a MAX3010 and DS18B20 sensors via an ESP32 microprocessor. The DS18B20 sensor is used to track body temperature, while the MAX3010 sensor measures pulse rate and oxygen saturation. The used antenna has a simple shape and can work at 2.8–8.7 GHz.

The following part will include antenna design in Section 2, return loss results from antenna simulation in Section 3.1, performance of antenna radiation patterns in Section 3.2, wearable device fabrication in Section 4, and conclusions in Section 5.

2. ANTENNA DESIGN

This study employs a Vivaldi antenna that operates in the UWB spectrum. Antenna designs in UWB technology have a fractional bandwidth greater than 0.2. The simulation employs felt as the substrate material, and there are two types of patches: copper tape and shieldit. The dimensions of the Coplanar Vivaldi Antenna design are $50 \times 50\,\text{mm}^2$, as shown in Table 2. Figure 1 shows the basic geometry of the Vivaldi antenna, with substrate thicknesses 1 and 3 mm.

TABLE 2. A sample table.

Par.	Dim. (mm)	Par.	Dim. (mm)	Par.	Dim. (mm)
L	50	Tr	21	PF	15
W	50	Cs	22.3	DF	4
Ws	40	r	15	LF	4
sL	2	pL	15.2	WF	125
rd	7	D	2.5	ZF	5.9

The slope of the patch on the front and the entire left and right sides corresponds to Equation (1) [22].

$$y = C_1 \cdot e^{Rx} + C_2,$$
$$C_1 = \frac{y_2 - y_1}{e^{Rx_2} - e^{Rx_1}}, \quad (1)$$
$$C_2 = \frac{y_1 e^{Rx_2} - y_2 e^{Rx_1}}{e^{Rx_2} - e^{Rx_1}}$$

In Equation (1), y is the coordinate of the point that forms the slope of the tapered slot, and its value is based on the constants C_1 and C_2. x_1, y_1 and x_2, y_2 are the coordinates of the start point and end point that will form a tapered slot line. The points y_1, y_2 are determined based on the initial slot width and the final slot opening width. R indicates the slope of the tapered slot. The greater the R value is, the steeper the slope is and vice versa. The direction of slope curvature also depends on determining the start and end points of the slope as well as the positive or negative sign of the constant R.

3. RESULTS AND DISCUSSION

3.1. The Return Loss Performance

Figure 2 displays the antenna's return loss performance with a felt substrate of thicknesses 1 mm and 3 mm. We demonstrate the return loss performance using two materials: copper tape and shieldit in the frequency range of 1 to 10 GHz. It indicates that such antennas reach S_{11} performance at -10 dB between 2.6 GHz and 8.7 GHz for the felt substrate with thickness 1 mm. However, the working frequencies with S_{11} below -10 dB when utilizing a 3 mm thick felt substrate are 4.6 GHz to 5.2 GHz and 8.2 to 8.6 GHz. The criteria for an ultra-wideband antenna has a fractional bandwidth value $>$ 20% [29, 30]. However, this antenna has an impedance bandwidth of 107% when the substrate thickness is 1 mm and a fractional bandwidth of 18.23% when the thickness is 3 mm. Differences in substrate thickness affect the working frequency range and have an impact on fractional bandwidth. However, the differences in patch materials do not significantly differ in S_{11} performance. It is evident that, given the same substrate thickness, the operating frequency of patches constructed from copper tape and shieldit is nearly identical. Because the fractional bandwidth for a substrate thickness of 1 mm is greater than that for a thickness of 3 mm, for the next simulation stage we fabricate a substrate with a thickness of 1 mm in a patch material.

The reflection coefficient based equivalent circuit of the proposed Vivaldi antenna is presented in Figure 3. The reflection coefficient consists of three bands, i.e., two passbands and one stopband. The passband ranges from 2.80 GHz to 3.40 GHz with resonance at 3.05 GHz, while the other passband ranges from 4.32 GHz to 8.79 GHz, and it resonates at three tuned frequencies 4.995 GHz, 6.50 GHz, and 8.21 GHz, respectively within the band. The stopband has a notch band ranging from 3.40 GHz to 4.32 GHz, and it has its highest reflection coefficient magnitude at 3.78 GHz. The passband resonances are represented by series RLC circuit in parallel branch to the source while the stopband resonance behaves as the parallel RLC resonance based on the simple RLC resonance theory [1]. The values of the R, L and C parameters are estimated using the series and parallel resonance conditions based on the quality factor, resonance frequencies, and their bands bandwidths as shown in Figure 3 [31]. The proposed circuit is simulated using Advanced Design System (ADS) software and then tuned at

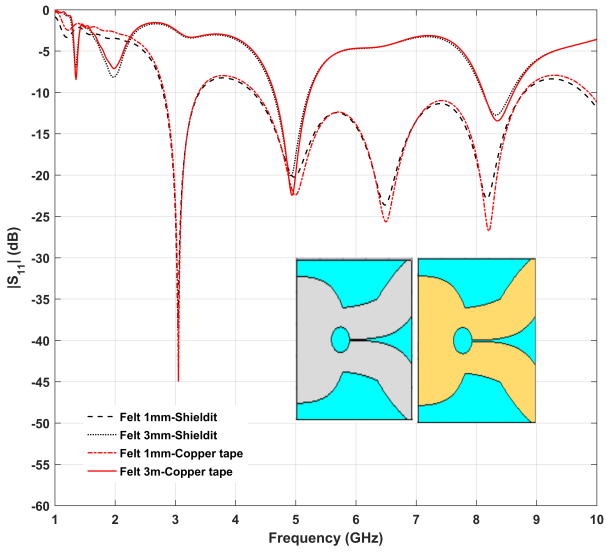

FIGURE 2. Return loss simulation results for patch materials copper tape and Shieldit.

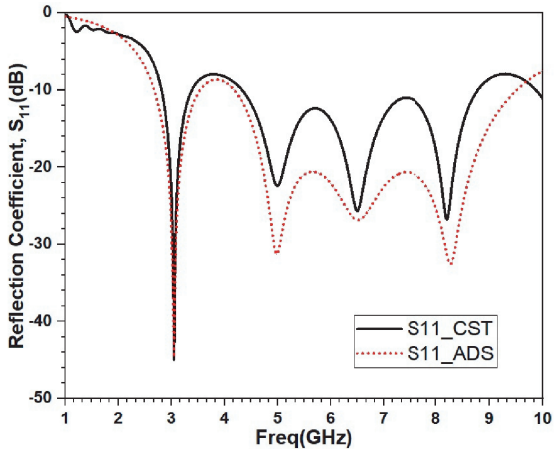

FIGURE 3. The reflection coefficients of textile coplanar Vivaldi antenna.

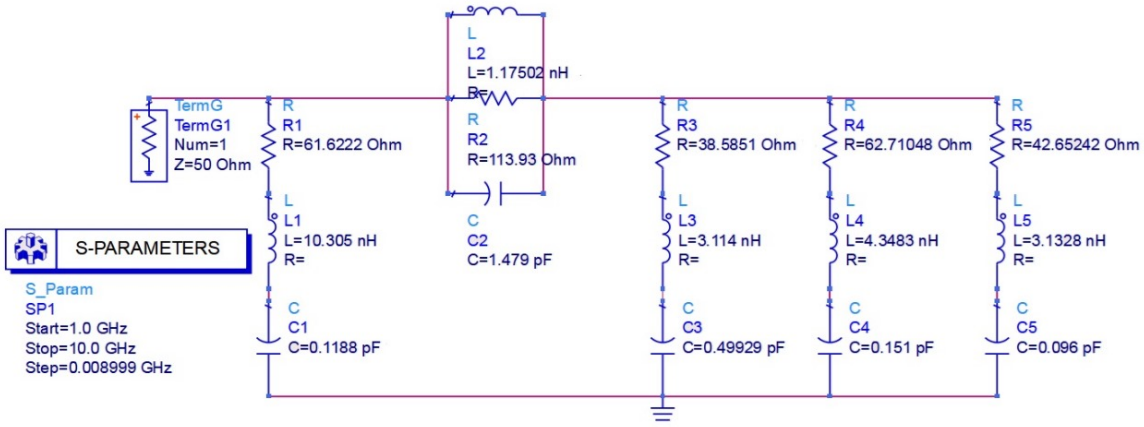

FIGURE 4. The equivalent circuit of textile coplanar Vivaldi antenna.

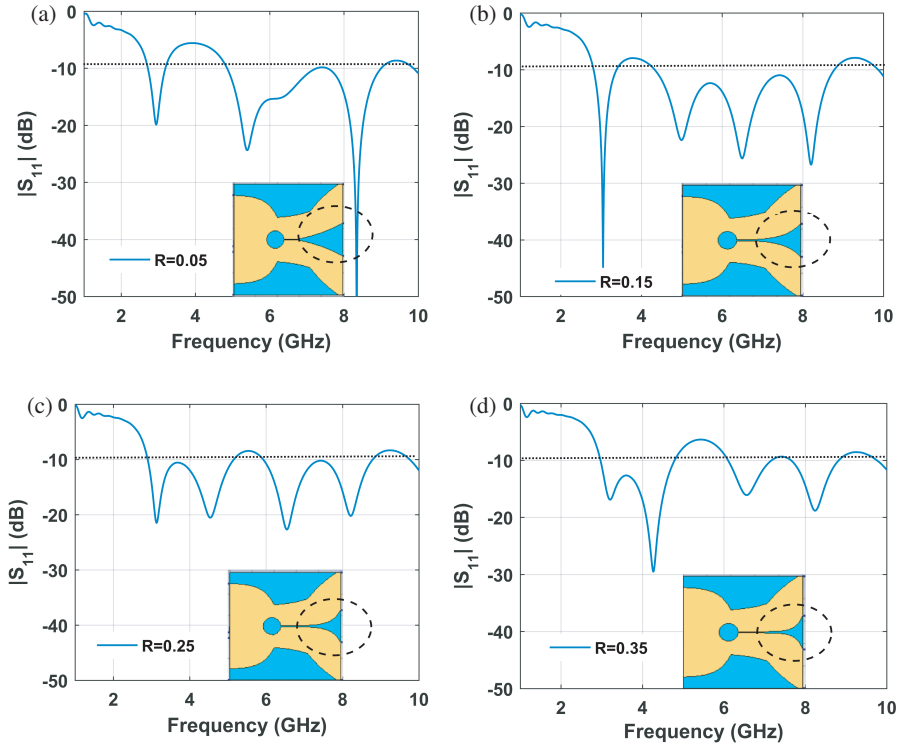

FIGURE 5. The reflection coefficients performance with variations slope (R) at the front opening of tapered slot antenna: (a) $R = 0.05$, (b) $R = 0.15$, (c) $R = 0.25$, and (d) $R = 0.35$.

the peak's resonances according to the simulated reflection coefficient of Computer Simulation Technology (CST) software designed antenna. The reflection coefficients of ADS designed antenna are found in excellent match in the lowest band while in the upper band the tuning frequencies are promising with the simulated design with little variations in the upper limit of the second band bandwidth. The comparisons of two reflection coefficients validated the circuit with proposed simulated antenna as shown in Figure 4 [32, 33].

Variations in the slopes of the tapered slot at the front aperture of the Vivaldi antenna and at both of its edges result in different return loss performances, as seen in Figures 5 and 6. At 8.33 GHz, the antenna's best resonance is -47.6 dB when $R = 0.05$, while at 3.07 GHz, it is -31.81 dB when $R = 0.15$. Nearly every frequency listed below produces S_{11} that is less than -10 dB when $R = 0.25$. At 4.29 GHz, the optimal resonance for $R = 0.35$ is -29.18. Concurrently, as illustrated in Figure 6, altering the antenna's two edge curves (Rc) causes several variations in the resonance frequency. Without utilizing a phantom, Figure 7 shows how variations in the antenna's bending radius affect S_{11} performance. It is evident that it performs poorly at 3 GHz for bending $R = 10$ mm. The optimal resonance is -44 dB at a frequency of 5 GHz if the antenna is bent with $R = 40$ mm, whereas the optimal resonance at 3 GHz is achieved by an antenna without bending (Normal). Bending will impact the antenna's operating frequency.

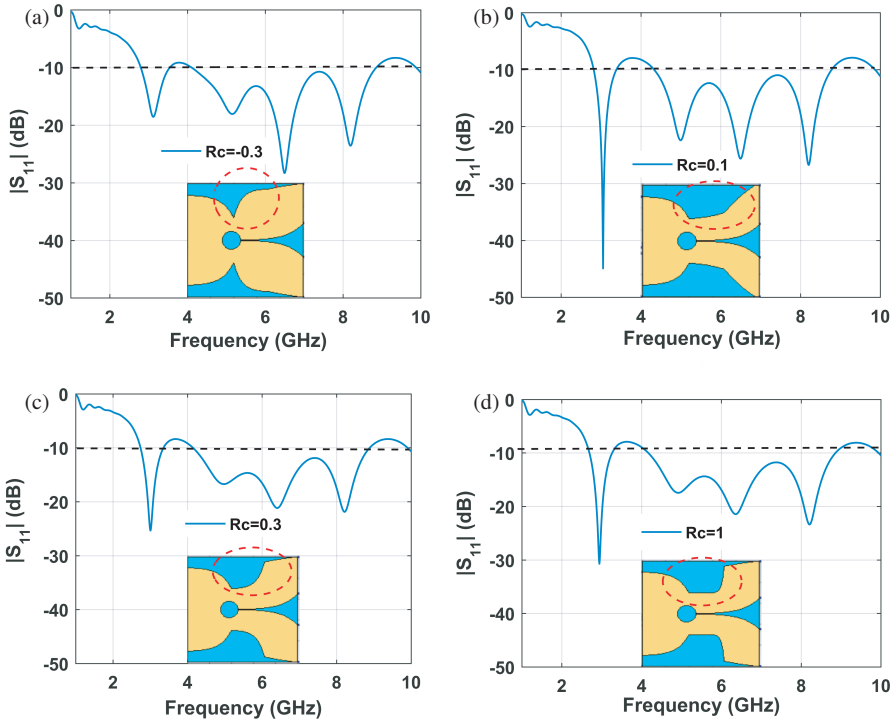

FIGURE 6. The reflection coefficients performance with variations slope (Rc) on both sides of the antenna edge: (a) $Rc = -0.3$, (b) $Rc = 0.1$, (c) $Rc = 0.3$, and (d) $Rc = 1$.

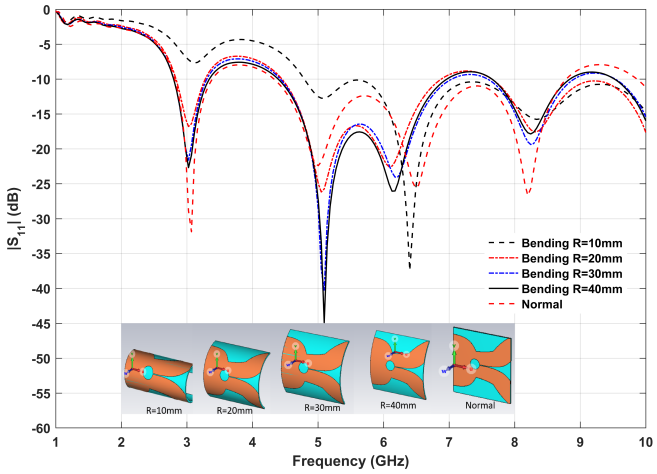

FIGURE 7. Directivity performance with R variations at the front of the tapered slot antenna.

3.2. The Radiation Pattern Performance

A radiation pattern is a graphical representation of the radiation qualities or form of an antenna's far-field output as a function of direction. Figure 8 depicts the antenna's far-field performance with Rc changing at frequencies of 3 and 7 GHz. At a frequency of 3 GHz, $R = -0.3$, the antenna generates a main lobe of 1.94 dBi, main lobe direction 0 deg, angular width (3 dB) $= 90.44°$, and sidelobe level (SLL) -1.0 dB. Meanwhile, for $Rc = 1$ at 3 GHz, the antenna generates a main lobe of 4.29 dBi, a main lobe direction of 0°, an angular width (3 dB) of 67.3°, and an SLL of -2.1 dB. Figure 8(a) shows that the antenna gain $Rc = 1$ is 2.63 dB larger than $Rc = -0.3$ at 3 GHz. However, antennas with $Rc = 1$ have a lower angular width and SLL than antennas with $Rc = -0.3$. Figure 8(b) depicts the far field at a 7 GHz frequency. The findings show that $Rc = -0.3$ is a superior antenna gain compared to $Rc = 1$. At $f = 7$ GHz and $Rc = 1$, the main lobe is 5.28 dBi; the angular width (3 dB) is 58.2°; and SLL is -4.9 dB. Meanwhile, for $R = -0.3$, the main lobe is 6.47 dBi; the main lobe direction is 0°; angular width (3 dB) $= 48.9°$; and SLL is -7.6 dB. So it can be seen that there is a gain difference of 1.19 dBi. From the simulation results, it is found that the SLL for $R = -0.3$ is better than the SLL at $R = 1$.

Vivaldi antennas provide a directed radiation pattern. Directional antennas are a type of antenna with a transmitting angle and power signal that is more directed in a certain direction. Meanwhile, an omnidirectional antenna is an antenna that has a signal transmission pattern with the same power in all directions. From Figure 8, it can be seen that the coplanar Vivaldi antenna tends to point at an angle of 0°. So this antenna has a directional radiation pattern even though when $R = 0.3$ at the frequency 3 GHz, it has a radiation pattern similar to an omnidirectional radiation pattern. It has a wide SLL, backlobe and beamwidth, but this antenna still has a main lobe which is still larger than the sidelobe and main lobe pointing to 0°. The polar plot of the antenna with $Rc = 1$ exhibits higher directivity than the antenna with $Rc = 0.3$, as shown in Figure 8(a). The radiation pattern with $Rc = 0.3$ has a broader beamwidth than the beamwidth with $Rc = 1$ because the antenna with $Rc = 0.3$ has a wider opening between the two taper slots than the one with $Rc = 1$. The antenna has a high SLL and backlobe, as

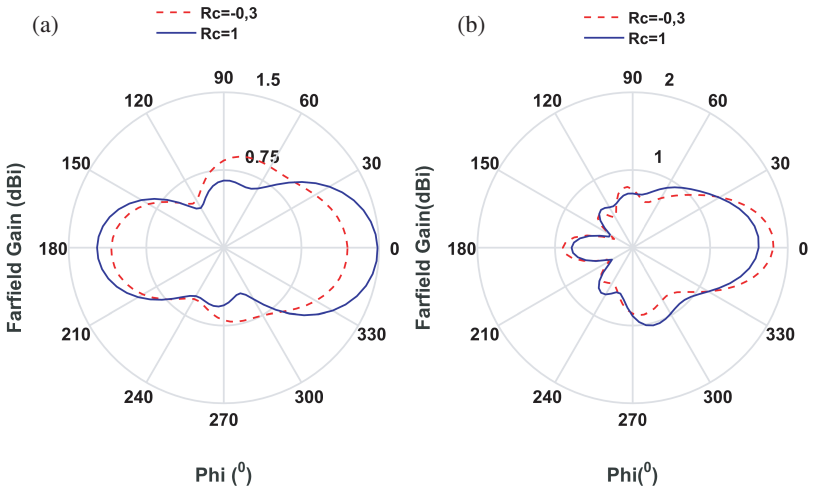

FIGURE 8. Far-field antenna with variations $Rc = -0.3$ and $Rc = 1$ when theta $= 90^{\circ}$ at frequencies of (a) 3 GHz and (b) 7 GHz.

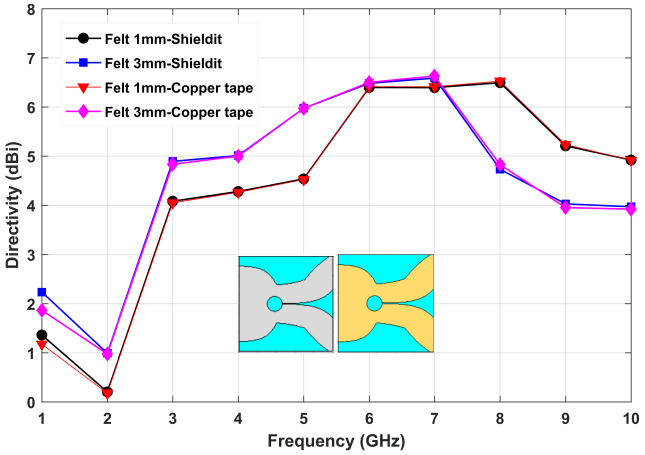

FIGURE 9. Directivity performance of coplanar Vivaldi textile antenna using felt substrate (thicknesses 1 and 3 mm) with copper tape and shieldit as patch materials.

shown in Figure 8(a). As a result, a technique to lower the SLL is required in order to increase the main lobe.

The variation of directivity with substrate material thickness is depicted in Figure 9, and variations in the slope R at the tapered slot opening and the slope Rc on both sides of the antenna edge are shown in Figures 10 and 11. Although we previously stated that we used a 1 mm substrate for the antenna because a 1 mm thick antenna performed better in S_{11} mode at almost all its operating frequencies (based on Figure 2), we also checked the directivity performance over antenna frequencies with varying substrate thicknesses, as shown in Figure 9. Nevertheless, in the directivity mode, a 3 mm thick substrate works better than a 1 mm thick antenna at frequencies lower than 7 GHz; however, this is not the case for frequencies higher than 7 GHz. In this case, we focus on the S_{11}'s performance rather than the directivity it generates. Therefore, these findings may serve as an example for incorporating further techniques to boost the antenna's directivity at the anticipated target frequency.

Meanwhile, Figure 10 demonstrates the change in antenna directivity caused by R modifications. By varying R, i.e., $R = 0.05$, $R = 0.15$, $R = 0.25$, and $R = 0.35$, the antenna has almost constant directivity of 1 to 4 GHz. Meanwhile, at frequencies greater than 5 GHz, the antenna with the biggest aperture tapered slot, in this case, for the smallest R-value, $R = 0.05$, has higher directivity than other R values. At 8 GHz, the antenna directivity is 6.8 dBi. Furthermore, Figure 11 displays antenna directivity as a function of Rc. In Figure 10 and 11, a coplanar Vivaldi antenna is designed using 0.017-mm-thick copper tape for the patch and feeding and 1 mm of felt for the substrate. The four values of Rc that are utilized are $Rc = -0.3$, $Rc = 0.1$, $Rc = 0.3$, and $Rc = 1$. The highest directivity reached at $Rc = -0.3$ at 6.98 dBi was determined from the simulation results. The antenna directivity is affected by the difference in R values.

The Vivaldi antenna distributes an electric field between two tapper slots. Figure 12 shows the difference in the surface current distribution between the textile antenna with felt substrate and the patch of copper tape and shieldit. Antennas with patches in the form of copper tape have a surface current distribution that is more concentrated between opening tapered slots than antennas with patches in the form of shieldit.

Because this study employs a textile antenna, Specific Absorption Rate (SAR) analysis is required before it can be used in wearable devices. SAR refers to the maximum amount of electromagnetic field that the human body can absorb. SAR can be formulated according to Equation (2) [10]

$$SAR = \sigma \frac{E^2}{\rho} \tag{2}$$

where σ refers to the tissue's conductivity expressed in units (S/m), E the intensity of the electric field in units V/m, and ρ the biological tissue density expressed in kg/m^3.

According to rules, the safe SAR limit for human health is less than 2 W/kg. We perform SAR analysis by simulating antennas over the skin (1 mm), fat (3 mm), and muscle (10 mm)

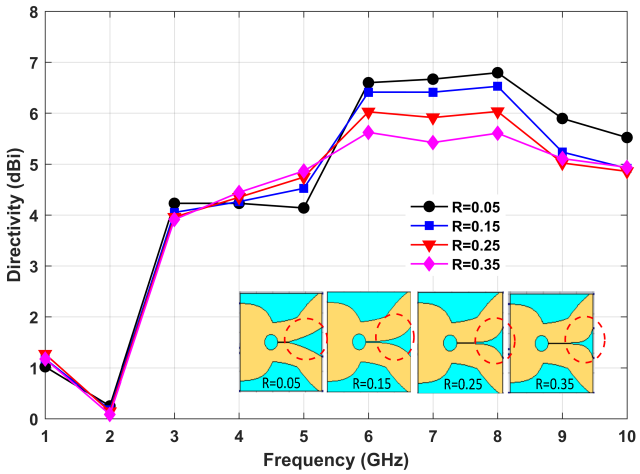

FIGURE 10. Directivity performance with R variations at the front of the tapered slot antenna.

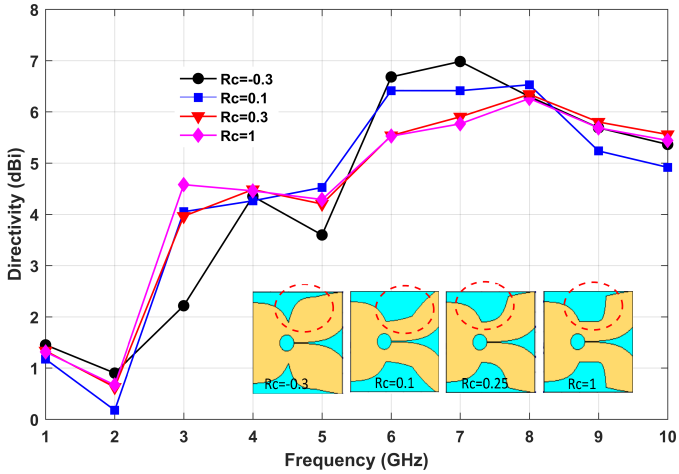

FIGURE 11. Directivity performance with variations in Rc slope on both sides of the antenna edge.

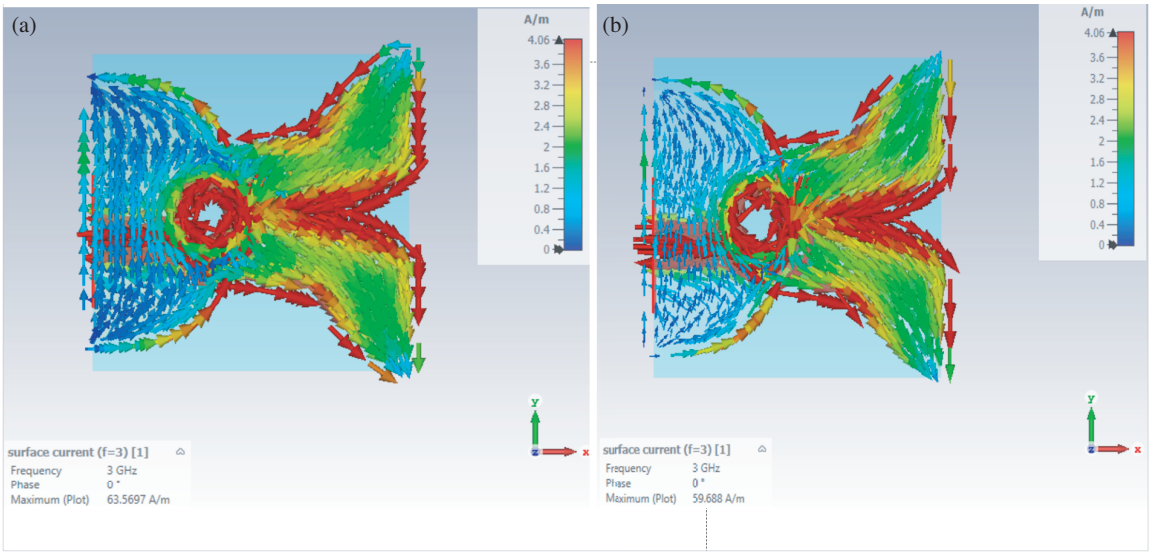

FIGURE 12. Surface Current on the 3 GHz frequency. (a) Copper tape. (b) Shield.

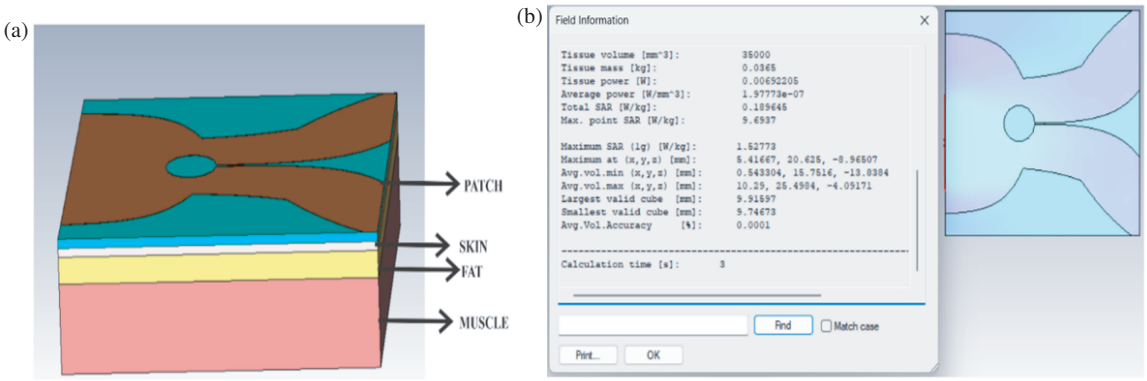

FIGURE 13. SAR simulation.

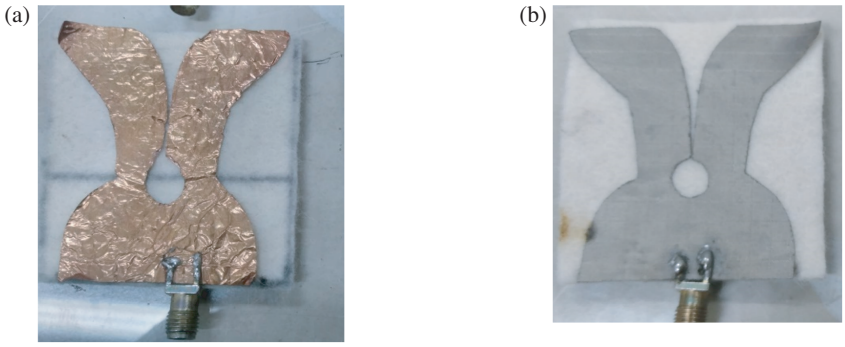

FIGURE 14. Fabrication results of 1 mm felt substrate with patch. (a) Copper tape (1 mm), and (b) shieldit (1 mm).

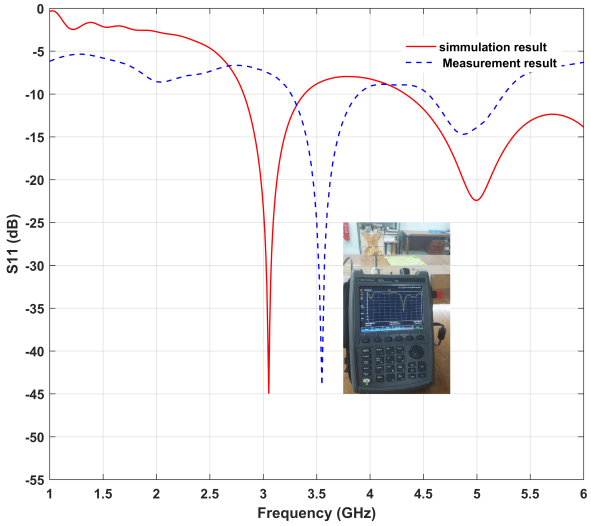

FIGURE 15. Comparison of simulation results and measurement results.

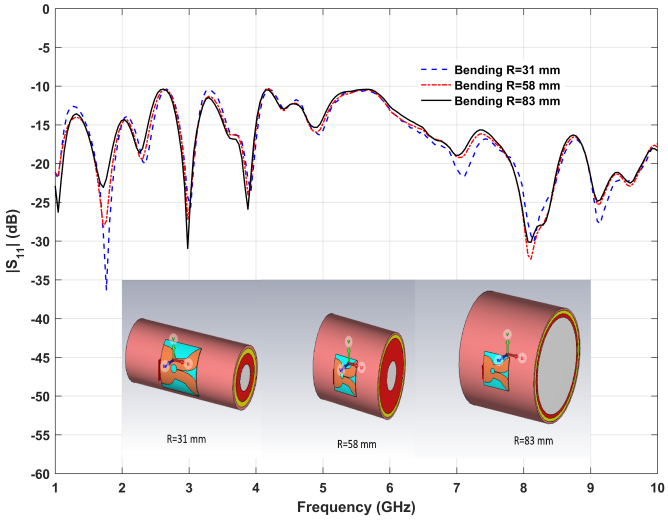

FIGURE 16. Return Loss measurement Results in different regions of the body.

of the human body as shown in Figure 13. The criteria of phantom are based on Table 3 [34]. However, the thickness can be changed depending on the body size. The simulation results revealed that the SAR values of the antenna with a patch in the shape of a copper tape were 1.52 W/kg. So we may infer that the coplanar Vivaldi antenna design employing textile materials fulfills the allowable SAR.

TABLE 3. Features of the phantom model.

Tissue	Thickness (mm)	permitivity	conductivity (mm)
Skim	2	69.45	0.507
Fat	10	6.07	0.036
Muscle	30	65.97	0.708

4. FABRICATION RESULT

The fabrication process was carried out using a felt substrate, copper tape, and shieldit as seen in Figure 14. After that, measurements were carried out using a portable Agilent VNA with a frequency up to 6 GHz as shown in Figure 15. There has also been a comparison between simulation and measurement results, as well as the S_{11} measurement procedure employing VNA in [35]. It is known from the measurement findings that the measurement results of felt and copper tape textile antenna differ slightly from the modeling results, demonstrated by the S_{11} measurement results, which shift to the right. The difference in simulation and measurement results can be caused by the fact that during the measurements, the portable VNA used had a maximum frequency of 6 GHz, while the maximum frequency used during the simulation was 10 GHz. Aside from that, differences in performance can also be caused because when making the antenna there is an air gap between the substrate material (felt) and the conductive patch (copper tape) where the two materials are joined together using adhesive, and there are several parts of the air gap that are not taken into account when modeling the antenna. At numerous frequencies, the S_{11} is less than -10 dB, indicating that the antenna has good bandwidth impedance, according to the measurement results.

The comparison of the S_{11} performance of a textile antenna bent in a phantom with several radii is shown in Figure 16. We

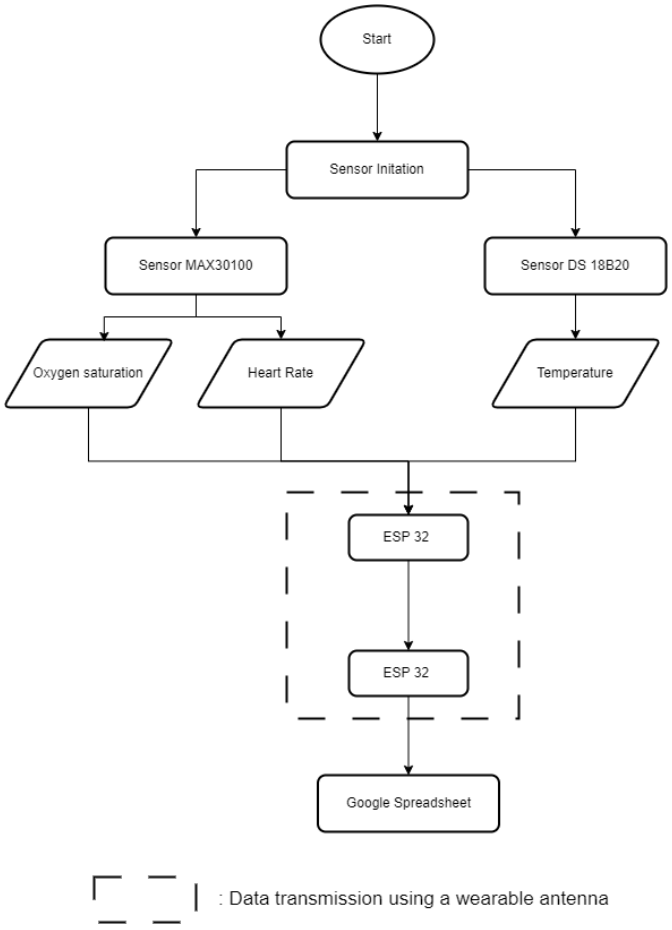

FIGURE 17. Working principle of wearable devices.

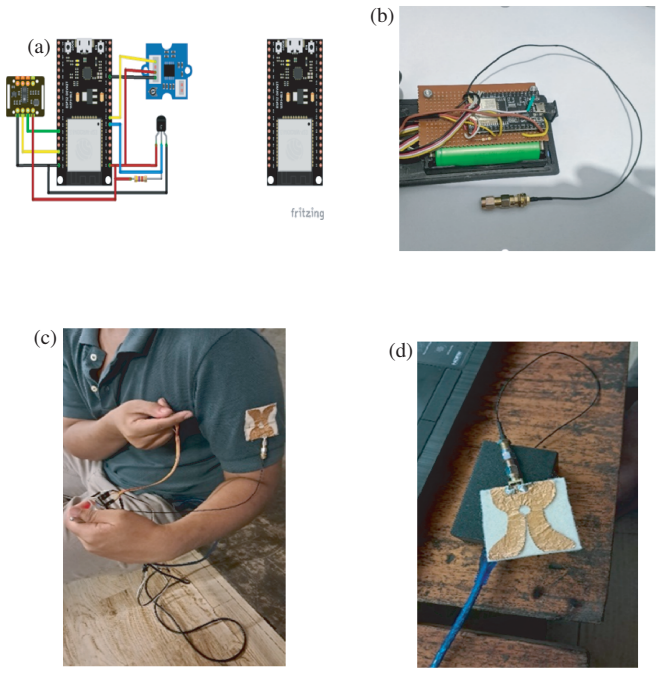

FIGURE 18. Wearable device: (a) Wiring diagram, (b) Device assembly, (c) Antenna testing on arm, and (d) Fabricated antenna on the wearable device.

used a cylindrical phantom with a variable radius to substitute the experimental images with simulation findings. This is to illustrate the thickness of the phantom in the form of bone, muscle, fat, and skin with different thicknesses between positions on the arm and thigh and also depending on the body size of the person using it. The dielectric constant and phantom thickness also depend on the position of the antenna and body condition at the time of measurement. From the simulation results using a phantom and bending the antenna following the phantom radius, it was found that the performance of the S_{11} antenna from 1 to 10 GHz mostly meets below -10 dB.

This study investigates the use of textile antennas in wearable devices. Figure 17 depicts the working principle of the wearable device. There are two sensors used: MAX30100 and DS18B20. Data from the MAX30100 sensor was used to monitor heart rate (BPM) and blood oxygen levels (SpO2). The DS18B20 sensor detects the body temperature and obtains temperature data by placing the sensor into the hand. The acquired sensor data is processed by an ESP 32 microcontroller and sent via a textile antenna as the antenna transmitter. The textile antenna on the receiver will receive data from the TX, and the results will be presented in the form of a Google spreadsheet. Figure 18 depicts the electronic circuit of the wearable device for the MAX30100 sensor, which is connected at pin 7 and for the DS18B20 sensor.

The wearable device is powered by two 3.7 V lithium batteries connected in series, and it has a charging connector. The textile antenna testing was carried out with Line of Sight (LOS) between the transmitter and receiver, and it was found that the transmitter could transmit body sensor data in the form of oxygen saturation, heart rate, and temperature with a delay of less than 1 minute to a distance of 10 meters as demonstrated in Figure 19. Figure 19(a) indicates that the oxygen saturation measurement varies every 30 seconds, and it is approximately 96%; however at 16.21.44 and 16.21.59, the oxygen saturation reading is zero, indicating that the data transmission mechanism suffers from little connection. However, the oxygen saturation reading looked to return to normal. The process of sending oxygen saturation data failed twice at several data collection times every 30 seconds. This can be caused by a loose installation of the oxygen saturation sensor, or a connection problem between the microcontroller and the wearable antenna. To increase transmission efficiency, it is necessary to pay attention to the integration of all components including sensors and transmitter devices that are properly installed, antenna placement, and increasing antenna performance in terms of bandwidth and gain. However, overall the success of sending oxygen saturation data was 93.1%. Heart rate values based on changes in time fluctuate between 77 bpm and 96.6 bpm, with an average heart rate of 88.7 bpm which is explored in Figure 19(b). For temperature readings as shown in Figure 19(c), at some initial times the temperature readings looked stable, namely 33.9°C; however after 16.20.52, the temperature readings became a minimum of 33.9° for a few moments, and the temperature readings increased to 34.2°. From the readings of the wearable device using the coplanar Vivaldi antenna as transmitter and receiver,

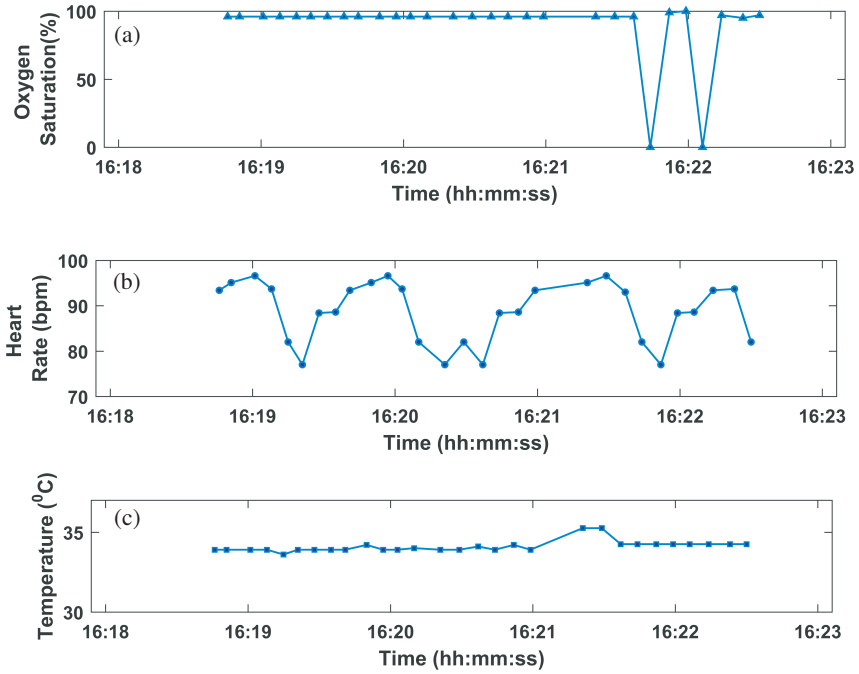

FIGURE 19. Data transmission results: (a) Oxygen Saturation, (b) Heart Rate and (c) Body Temperature.

it can be seen that data transmission can be carried out well, but it may be necessary to calibrate the measuring instrument with a standard measuring instrument. Apart from being in graphical form, the data may also be shown in table form in the form of a Google spreadsheet.

Table 4 shows a reference comparison table related to wearable antennas. In Table 4, [14] employs felt material and has a smaller size and SAR than all the references in Table 4, but the bandwidth percentage of this antenna is only 61.69%, whereas the antenna we built has a fractional bandwidth of 107.14%. Antennas [35–37] built from Denim, Tachonic, and jeans substrate materials have a lower bandwidth than the antennas we created. Ref. [38] investigated an antenna that can operate at lower frequencies than the one we built but is bigger in size and has a modest fractional bandwidth 12.5%. The antenna in [39, 40] is compact and made of shieldit, yet it has a narrow fractional bandwidth of 12.7% and 14.5%, respectively. Ref. [41] has a slightly bigger size than the antenna we built and a fractional bandwidth of 15.3%, but [42] and [43], despite having a lower SAR value, have a larger antenna and fractional bandwidth. The lesser percentages are 2.11% and 12%. The antenna that we build has a bandwidth around 107.14%.

From the table it can be seen that the antenna made has wider bandwidth performance than other wearable antennas. Based on the previous discussion, it is possible to infer that coplanar Vivaldi antennas manufactured from textile materials, namely a 1 mm thick substrate material and patch materials in the form of copper tape and shieldit, can be utilized to transmit body data via a wearable device.

TABLE 4. Comparison of previously published reference.

Ref.	Textile	Dim. (mm^2)	Freq. (GHz)	SAR W/kg
[14]	Felt	55 × 34	1.76–3.33	0.01
[35]	Denim	35.4 × 82.4	2.39–2.54	0.297
[36]	Tachonic	48.7 × 42	1.8–2.6	1.48
[37]	Jeans	40 × 50	3.6–7	1.93
[38]	Polyester	90 × 100	1.5–1.7	-
[39]	Shieldit	12.5 × 12.5	2.2–2.5	-
[40]	opper	12.5 × 12.5	4.4–5.8	0.12
[41]	Embroider	53 × 53	2.4–2.8	2.78
[42]	Polyester	66 × 66	2.34–2.39	0.47
[42]	Denim,	180 × 120	2.2–2.5	0.15
This Work	Felt Copper	50 × 50	2.6–8.7	1.52

5. CONCLUSION

This research develops a textile coplanar Vivaldi antenna using a felt substrate with two patch materials, namely copper tape and shieldit. From the simulation results, it was found that the antenna can work at frequencies from 2.8 GHz to 8.7 GHz with a minimum return loss value of −44 dB at a frequency of 3 GHz. Varying the slope of the tapered slot on the front and side of the antenna increases directivity. This study has also created a wearable monitoring system by combining the MAX30100 and DS18B20 sensors and delivering data via an ESP32 microprocessor attached to a textile antenna. The antenna can convey data from the heart rate sensor between 77 and 96 BPM, oxygen saturation between 96 and 100%, and body temperature between 31.25 and 34.25°C. The data is delivered up to 10 meters, and data from the sensor may be shown in the form of

graphs and Google spreadsheets with a delay of less than one minute. As a result, the coplanar Vivaldi textile antenna design may be suggested for future health monitoring equipment development.

ACKNOWLEDGEMENT

We appreciate the funds granted by the DRTPM (Directorate of Research, Technology, and Community Service) KEMENDIKBUDRISTEK Decree No. 145/E5/PG.02.00.PL/2023 and No. 071/E5/PG.02.00.PL/2024 and Universitas Negeri Surabaya.

REFERENCES

[1] Hoang, V.-P., V.-L. Dao, and V.-B. Dang, "Temperature beat sensor for energy efficient, long range smart monitoring systems," in *2020 International Conference on Green and Human Information Technology (ICGHIT)*, 18–20, Hanoi, Vietnam, Feb. 2020.

[2] Sabban, A., "Small new wearable antennas for IOT, medical and sport applications," in *2019 13th European Conference on Antennas and Propagation (EuCAP)*, 1–5, Krakow, Poland, Mar. 2019.

[3] Sharif, A., J. Guo, J. Ouyang, K. Arshad, M. A. Imran, and Q. H. Abbasi, "Ultra-wideband sensor antenna design for 5G/UWB based real time location systems," in *2020 International Workshop on Antenna Technology (iWAT)*, 1–4, Bucharest, Romania, Feb. 2020.

[4] Sreelekshmi, S. and S. P. Sankar, "Performance comparison of wearable antennas for body centric wireless communication," in *2018 International Conference on Emerging Trends and Innovations In Engineering And Technological Research (ICETIETR)*, 1–4, Ernakulam, India, Jul. 2018.

[5] Çelenk, E. and N. T. Tokan, "All-textile on-body antenna for military applications," *IEEE Antennas and Wireless Propagation Letters*, Vol. 21, No. 5, 1065–1069, 2022.

[6] Sipal, V., D. Gaetano, P. McEvoy, and M. J. Ammann, "Impact of hub location on the performance of wireless body area networks for fitness applications," *IEEE Antennas and Wireless Propagation Letters*, Vol. 14, 1522–1525, 2014.

[7] Bhatti, D. S., S. Saleem, A. Imran, Z. Iqbal, A. Alzahrani, H. Kim, and K.-I. Kim, "A survey on wireless wearable body area networks: A perspective of technology and economy," *Sensors*, Vol. 22, No. 20, 7722, 2022.

[8] Wang, H., Z. Zhang, Y. Li, and Z. Feng, "A dual-resonant shorted patch antenna for wearable application in 430 MHz band," *IEEE Transactions on Antennas and Propagation*, Vol. 61, No. 12, 6195–6200, 2013.

[9] Gao, G.-P., C. Yang, B. Hu, R.-F. Zhang, and S.-F. Wang, "A wearable PIFA with an all-textile metasurface for 5 GHz WBAN applications," *IEEE Antennas and Wireless Propagation Letters*, Vol. 18, No. 2, 288–292, 2019.

[10] Kavitha, K., S. R. V. Gokul, S. Yazhini, J. M. K. Durga, and R. Keerthana, "EBG integrated metasurface antenna for SAR reduction," *Progress In Electromagnetics Research C*, Vol. 135, 227–240, 2023.

[11] Gao, G.-P., B.-K. Zhang, J.-H. Dong, Z.-H. Dou, Z.-Q. Yu, and B. Hu, "A compact dual-mode pattern-reconfigurable wearable antenna for the 2.4-GHz WBAN application," *IEEE Transactions on Antennas and Propagation*, Vol. 71, No. 2, 1901–1906, 2022.

[12] Le, T. T., Y.-D. Kim, and T.-Y. Yun, "All-textile enhanced-bandwidth polarization-conversion antenna using a nonuniform metasurface," *IEEE Antennas and Wireless Propagation Letters*, Vol. 22, No. 10, 2432–2436, 2023.

[13] Xu, Y., L. Mu, Y. Xu, A. Mahmoud, Y. Wang, and O. M. Ramahi, "Wearable directional button antenna for on-body wireless power transfer," *Electronics*, Vol. 12, No. 8, 1758, 2023.

[14] Hashim, F. F., W. N. L. B. W. Mahadi, T. B. A. Latef, and M. B. Othman, "Fabric-metal barrier for low specific absorption rate and wide-band felt substrate antenna for medical and 5G applications," *Electronics*, Vol. 12, No. 12, 2754, 2023.

[15] Ali, W., N. Nizam-Uddin, W. M. Abdulkawi, A. Masood, A. Hassan, J. A. Nasir, and M. A. Khan, "Design and analysis of a quad-band antenna for IoT and wearable RFID applications," *Electronics*, Vol. 13, No. 4, 700, 2024.

[16] Salonen, P., Y. Rahmat-Samii, M. Schaffrath, and M. Kivikoski, "Effect of textile materials on wearable antenna performance: A case study of GPS antennas," in *IEEE Antennas and Propagation Society Symposium, 2004.*, Vol. 1, 459–462, Monterey, CA, USA, Jun. 2004.

[17] Zhu, S. and R. Langley, "Dual-band wearable antennas over EBG substrate," *Electronics Letters*, Vol. 43, No. 3, 1–2, 2007.

[18] Locher, I., M. Klemm, T. Kirstein, and G. Troster, "Design and characterization of purely textile patch antennas," *IEEE Transactions on Advanced Packaging*, Vol. 29, No. 4, 777–788, 2006.

[19] Scarpello, M. L., I. Kazani, C. Hertleer, H. Rogier, and D. V. Ginste, "Stability and efficiency of screen-printed wearable and washable antennas," *IEEE Antennas and Wireless Propagation Letters*, Vol. 11, 838–841, 2012.

[20] Kumar, A., A. Utsav, and R. K. Badhai, "A novel copper-tape wideband wearable textile antenna for WBAN applications," in *2017 IEEE Applied Electromagnetics Conference (AEMC)*, 1–3, Aurangabad, India, Dec. 2017.

[21] Rambe, A. H., M. Jusoh, S. S. Al-Bawri, and M. A. Abdelghany, "Wearable UWB antenna-based bending and wet performances for breast cancer detection," *Computers, Materials & Continua*, Vol. 73, No. 3, 5575–5587, 2022.

[22] Nurhayati, N., F. Y. Zulkifli, E. Setijadi, B. E. Sukoco, M. N. M. Yasin, and A. M. D. Oliveira, "Bandwidth, gain improvement and notched-band frequency of SWB wave coplanar Vivaldi antenna using CSRR," *IEEE Access*, Vol. 12, 16 926–16 938, 2024.

[23] Nurhayati, N., E. Setijadi, and M. N. M. Yasin, "Coplanar Vivaldi antenna with wave slot structure for RADAR application," in *2022 IEEE International Conference on Communication, Networks and Satellite (COMNETSAT)*, 247–251, Solo, Indonesia, Nov. 2022.

[24] Le, T. T. and T.-Y. Yun, "Miniaturization of a dual-band wearable antenna for WBAN applications," *IEEE Antennas and Wireless Propagation Letters*, Vol. 19, No. 8, 1452–1456, 2020.

[25] Velan, S., E. F. Sundarsingh, M. Kanagasabai, A. K. Sarma, C. Raviteja, R. Sivasamy, and J. K. Pakkathillam, "Dual-band EBG integrated monopole antenna deploying fractal geometry for wearable applications," *IEEE Antennas and Wireless Propagation Letters*, Vol. 14, 249–252, 2014.

[26] Jhunjhunwala, V. K., T. Ali, P. Kumar, P. Kumar, P. Kumar, S. Shrivastava, and A. A. Bhagwat, "Flexible UWB and MIMO antennas for wireless body area network: A review," *Sensors*, Vol. 22, No. 23, 9549, 2022.

[27] Abd El-Hameed, A. S., D. M. Elsheakh, G. M. Elashry, and E. A. Abdallah, "A comparative study of narrow/ultra-wideband microwave sensors for the continuous monitoring of vital signs and lung water level," *Sensors*, Vol. 24, No. 5, 1658, 2024.

[28] Li, R. and Y. Guo, "A conformal UWB dual-polarized antenna for wireless capsule endoscope systems," *IEEE Antennas and Wireless Propagation Letters*, Vol. 20, No. 4, 483–487, 2021.

[29] Ahirwar, M. and V. S. Chaudhary, "Advancing wireless connectivity: A dual-band microstrip antenna enhanced by hexagon cell reflector for superior gain and directivity," *Progress In Electromagnetics Research M*, Vol. 124, 53–61, 2024.

[30] Nurhayati, N., A. M. De-Oliveira, W. Chaihongsa, B. E. Sukoco, and A. K. Saleh, "A comparative study of some novel wideband tulip flower monopole antennas with modified patch and ground plane," *Progress In Electromagnetics Research C*, Vol. 112, 239–250, 2021.

[31] Varshney, A., N. Cholake, and V. Sharma, "Low-cost ELC-UWB fan-shaped antenna using parasitic SRR triplet for ISM band and PCS applications," *International Journal of Electronics Letters*, Vol. 10, No. 4, 391–402, 2022.

[32] Varshney, A., V. Sharma, and A. K. Sharma, "RLC-equivalent circuit based stub loaded 2x2 MIMO antenna for wireless applications," *Microwave Review*, Vol. 29, No. 1, 2023.

[33] Varshney, A., V. Sharma, C. Nayak, A. K. Goyal, and Y. Massoud, "A low-loss impedance transformer-less fish-tail-shaped MS-to-WG transition for K-/Ka-/Q-/U-band applications," *Electronics*, Vol. 12, No. 3, 670, 2023.

[34] Sugunavathy, S., V. K. Sudha, and D. Parthiban, "Fabric woven textile antenna for medical applications," in *Journal of Physics: Conference Series*, Vol. 1917, No. 1, 012022, 2021.

[35] Ejaz, A., I. Jabeen, Z. U. Khan, A. Alomainy, K. Aljaloud, A. H. Alqahtani, N. Hussain, R. Hussain, and Y. Amin, "A high performance all-textile wearable antenna for wristband application," *Micromachines*, Vol. 14, No. 6, 1169, 2023.

[36] Dong, Y., H. Lu, and X. Chen, "A novel dual-band circularly polarized wearable antenna," *Micromachines*, Vol. 15, No. 5, 588, 2024.

[37] Pradeep, P., M. M. Basha, S. Gundala, and J. Syed, "Development of wearable textile MIMO antenna for sub-6 GHz band new radio 5G applications," *Micromachines*, Vol. 15, No. 5, 651, 2024.

[38] Zaidi, N. I., N. H. A. Rahman, M. F. Yahya, M. S. A. Nordin, S. Subahir, Y. Yamada, and A. Majumdar, "Analysis on bending performance of the electro-textile antennas with bandwidth enhancement for wearable tracking application," *IEEE Access*, Vol. 10, 31 800–31 820, 2022.

[39] Ashyap, A. Y. I., Z. Z. Abidin, S. H. Dahlan, H. A. Majid, A. M. A. Waddah, M. R. Kamarudin, G. A. Oguntala, R. A. Abd-Alhameed, and J. M. Noras, "Inverted E-shaped wearable textile antenna for medical applications," *IEEE Access*, Vol. 6, 35 214–35 222, 2018.

[40] Sharma, D., S. Kumar, R. N. Tiwari, H. C. Choi, and K. W. Kim, "On body and off body communication using a compact wideband and high gain wearable textile antenna," *Scientific Reports*, Vol. 14, No. 1, 14493, 2024.

[41] Martinez, I., C.-X. Mao, D. Vital, H. Shahariar, D. H. Werner, J. S. Jur, and S. Bhardwaj, "Compact, low-profile and robust textile antennas with improved bandwidth for easy garment integration," *IEEE Access*, Vol. 8, 77 490–77 500, 2020.

[42] Aprilliyani, R., P. A. Dzagbletey, J. H. Lee, M. J. Jang, J.-H. So, and J.-Y. Chung, "Effects of textile weaving and finishing processes on textile-based wearable patch antennas," *IEEE Access*, Vol. 8, 63 295–63 301, 2020.

[43] Atanasova, G. and N. Atanasov, "Small antennas for wearable sensor networks: Impact of the electromagnetic properties of the textiles on antenna performance," *Sensors*, Vol. 20, No. 18, 5157, 2020.